Matching NLR Immune Receptors to Autoimmunity in camta3 Mutants Using Antimorphic NLR Alleles

Lolle, Signe; Greeff, Christiaan; Petersen, Klaus; Roux, Milena; Jensen, Michael Krogh; Bressendorff, Simon; Rodriguez, Eleazar; Sømark, Kenneth; Mundy, John; Petersen, Morten

Published in:
Cell Host & Microbe

Link to article, DOI:
10.1016/j.chom.2017.03.005

Publication date:
2017

Document Version
Publisher's PDF, also known as Version of record

Article

Cell Host & Microbe

Matching NLR Immune Receptors to Autoimmunity in *camta3* Mutants Using Antimorphic NLR Alleles

Graphical Abstract

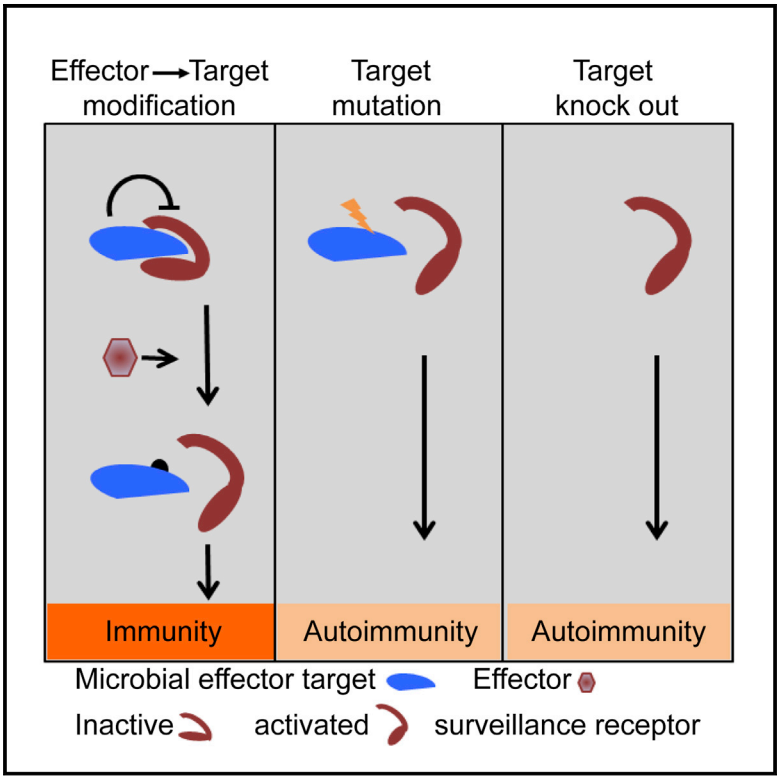

Authors

Signe Lolle, Christiaan Greeff, Klaus Petersen, ..., Kenneth Sømark, John Mundy, Morten Petersen

Correspondence

shutko@bio.ku.dk

In Brief

NLRs detect pathogen-induced modifications in plant proteins, triggering immunity. Lolle et al. express dominant-negative NLRs (DN-NLRs) and screen for suppressed autoimmunity in various mutants. DN-NLRs for DSC1 and DSC2 suppress autoimmunity in a *camta3* mutant, a putative negative regulator of immunity, suggesting that autoimmunity results from detection of modified self.

Highlights

- Dominant-negative NLR forms (DN-NLR) disrupt the function of wild-type NLR alleles
- DN-NLRs can be used to screen for suppression of autoimmunity in autoimmune mutants
- Two NLRs (DSC1 and DSC2) are responsible for autoimmunity in *Arabidopsis camta3* mutants
- Immunity triggered by DSC1 or DSC2 in tobacco is suppressed by CAMTA3 co-expression

Lolle et al., 2017, Cell Host & Microbe *21*, 518–529
April 12, 2017
http://dx.doi.org/10.1016/j.chom.2017.03.005

CellPress

Cell Host & Microbe
Article

Matching NLR Immune Receptors to Autoimmunity in *camta3* Mutants Using Antimorphic NLR Alleles

Signe Lolle,[1,3] Christiaan Greeff,[1,3] Klaus Petersen,[1] Milena Roux,[1] Michael Krogh Jensen,[1,2] Simon Bressendorff,[1] Eleazar Rodriguez,[1] Kenneth Sømark,[1] John Mundy,[1] and Morten Petersen[1,4,*]

[1]Department of Biology, University of Copenhagen, 2200 Copenhagen N, Denmark
[2]The Novo Nordisk Foundation Center for Biosustainability, Technical University of Denmark, 2800 Hørsholm, Denmark
[3]Co-first author
[4]Lead Contact
*Correspondence: shutko@bio.ku.dk
http://dx.doi.org/10.1016/j.chom.2017.03.005

SUMMARY

To establish infection, pathogens deploy effectors to modify or remove host proteins. Plant immune receptors with nucleotide-binding, leucine-rich repeat domains (NLRs) detect these modifications and trigger immunity. Plant NLRs thus guard host "guardees." A corollary is that autoimmunity may result from inappropriate NLR activation because mutations in plant guardees could trigger corresponding NLR guards. To explore these hypotheses, we expressed 108 dominant-negative (DN) *Arabidopsis* NLRs in various lesion mimic mutants, including *camta3*, which exhibits autoimmunity. CAMTA3 was previously described as a negative regulator of immunity, and we find that autoimmunity in *camta3* is fully suppressed by expressing DNs of two NLRs, DSC1 and DSC2. Additionally, expression of either NLR triggers cell death that can be suppressed by *CAMTA3* expression. These findings support a model in which DSC1 and DSC2 guard CAMTA3, and they suggest that other negative regulators of immunity may similarly represent guardees.

INTRODUCTION

The innate immune system includes receptors that recognize pathogen-associated molecular patterns (PAMPs). Thus, plants and animals have bacterial flagellin receptors that trigger immunity (Gómez-Gómez and Boller, 2002). Successful pathogens deliver effectors into host cells to suppress this layer of immunity (Jones and Dangl, 2006). In a next layer, cytoplasmic nucleotide-binding leucine-rich repeat domain (NLR) receptors, which are similar to animal NOD-like receptors, directly or indirectly recognize the activities of pathogen effectors. NLRs activate effector triggered immunity (ETI) that is often associated with local host cell death known as the hypersensitive response (HR) (Dangl et al., 2013). Two subfamilies of plant NLRs can be defined by the presence of either an N-terminal Toll/interleukin-1 receptor (TIR) or a coiled-coil (CC) domain (Jones and Dangl, 2006). Signaling by TIR-NLRs generally requires ENHANCED DISEASE SUSCEPTEBILITY1 (EDS1), whereas NON-RACE SPECIFIC DISEASE RESISTANCE1 (NDR1) is important for CC-NLR-triggered HR (Aarts et al., 1998). So while bacterial effectors possess diverse activities to manipulate host responses (Speth et al., 2007), NLRs with diverse recognition specificities and downstream signaling are found in single plant species (DeYoung and Innes, 2006). An example of this complexity is the bacterial pathogen *Pseudomonas syringae* (*Pst*), which injects effectors via a type III secretion system to establish infection in *Arabidopsis* (Buell et al., 2003). These effectors include AvrRpm1 and AvrRpt2, which target the host protein RIN4 by phosphorylation or degradation, respectively. These changes in RIN4 are detected by two NLRs, RPM1 and RPS2, which both trigger ETI (Axtell and Staskawicz, 2003; Belkhadir et al., 2004). Importantly, loss of RIN4 results in RPS2-dependent autoimmunity, indicating that RPS2 guards RIN4 (Axtell and Staskawicz, 2003; Spoel and Dong, 2012).

Numerous autoimmune or lesion mimic mutants are caused by gain-of-function mutations in NLRs (Shirano et al., 2002; Zhang et al., 2003) or by loss of function in diverse genes thought to act as negative regulators of immunity and the HR (Dietrich et al., 1994; Greenberg and Ausubel, 1993; Greenberg et al., 1994; Lu et al., 2011; Petersen et al., 2000; Shirano et al., 2002; Zhang et al., 2003). Interestingly, the autoimmune phenotypes of these mutants are largely the same as those for ETI, including EDS1/PAD4 or NDR1 dependency, stunted growth, accumulation of reactive oxygen species, and elevated defense gene expression (Brodersen et al., 2002, 2006; Grant et al., 2000; Sohn et al., 2014; Zhang et al., 2003). In addition, like ETI, autoimmunity can often be suppressed by high growth temperature (Zhang et al., 2012). Importantly, some 40% of *Arabidopsis* autoimmune mutants are suppressed by mutations in NLRs and other immune signaling components (Bruggeman et al., 2015; Rodriguez et al., 2016).

Other evidence linking autoimmunity and NLRs may be hybrid necrosis. Some 2% of intraspecific *Arabidopsis* crosses yield F1 progeny with hybrid necrosis or autoimmunity, which can be suppressed at higher growth temperatures (Bomblies and Weigel, 2007). These incompatibility loci often map to rapidly evolving *NLR* genes or gene clusters. Such hybrid necrosis may be due to the activation of NLR-dependent defense responses due to a failure in guard-guardee interactions (Chae et al., 2014).

In some instances, NLR-dependent autoimmunity is well described. ACCELERATED CELL DEATH11 (ACD11) is a ceramide-1-phosphate transfer protein (Simanshu et al., 2014), and *acd11* mutants exhibit autoimmunity dependent on the NLR LAZ5. Thus, *acd11* is rescued by *laz5* knockout and by a dominant-negative *laz5-D2* allele, indicating that ACD11 or its complexes/pathways are likely effector target(s) guarded by LAZ5 (Palma et al., 2010). The *laz5D-2* allele has a mutation in the P loop (Ile→Asn) of its nucleotide-binding domain (Palma et al., 2010). This is similar to the *DN* mutation (Val→Asn) of the tobacco *NLR N*, which also abolishes its function (Mestre and Baulcombe, 2006). Clearly, the P loop is important for NLR function.

Knockout of *MAP kinase 4* (*MPK4*) or double knockouts of the two upstream kinases *MKK1* and *2* also lead to autoimmunity, which is suppressed by mutations in the *NLR SUMM2.* Since the MPK4 pathway is a target of the HopAI1 effector and HopAI1 activity triggers SUMM2, loss of MKK1/2 mimics the presence of HopAI1 and triggers SUMM2-dependent autoimmunity (Zhang et al., 2012). It is, therefore, likely that NLRs cause autoimmunity in plants with mutations in genes encoding effector targets.

An example of such NLR-induced autoimmunity might be the CALMODULIN BINDING TRANSCRIPTION ACTIVATOR 3 (CAMTA3) with five homologs in *Arabidopsis* (CAMTA1–6) (Bouché et al., 2002). CAMTA1, 2, and 3 appear to coordinately regulate gene expression (Kim et al., 2013), but loss of CAMTA3 is sufficient to cause autoimmunity (Galon et al., 2008). Since CAMTA3 can bind to the promoter of *EDS1* and mutations in *EDS1* rescue *camta3* mutants, CAMTA3 was proposed to function as a negative regulator of immunity and *EDS1* transcription (Du et al., 2009). In contrast, CAMTAs may positively regulate early stress response genes via a core CAMTA-binding sequence present in their promoters (Benn et al., 2014).

We describe here a collection of 108 *Arabidopsis* NLRs mutated in their P loops to potentially create their corresponding dominant-negative NLR-DN alleles. We transform this collection into various lesion mimic mutants, including *camta3*, to screen for suppression of autoimmunity. As proof of principle, we first show that transgenic lines expressing *RPM1-DN* are indistinguishable from *rpm1–3* knockout mutants in terms of ETI and gene-for-gene resistance. Importantly, *RPM1-DN* does not interfere with common CC-NLR or TIR-NLR signaling pathways. In addition, we find that DN mutants of two NLRs we name *DSC1* and *DSC2* fully suppress autoimmunity in the *camta3* mutant. Since DSC1- and DSC2-triggered cell death in *N. benthamiana* is prevented specifically by *CAMTA3* expression and as DSC1 appears to interact with both CAMTA3 and DSC2, autoimmunity in *camta3* is probably not caused by a lack of its proposed function as a negative regulator of genes required for immunity. Instead, the *camta3* phenotype is triggered by the NLRs DSC1 and DSC2.

RESULTS

Function and Specificity of P Loop Mutations

Screens for suppression of one or more autoimmune mutants by NLR loss-of-function mutations are time consuming and potentially uninformative for NLRs with redundant functions. We therefore took an alternative, transgenic approach with a screen for suppression in T2 transformants. Since specific mutations in the P loop domain of NLRs can have dominant-negative effects (Dinesh-Kumar et al., 2000; Palma et al., 2010; Roberts et al., 2013), we examined the consequences of a P loop mutation in the well-studied CC-NLR RPM1 (GK,221,222,AA; here named *RPM1-DN*). RPM1 triggers cell death in plants infected with *Pst* DC3000 (AvrRpm1) (Grant et al., 1995). We compared cell death responses in 4-week-old Col-0, *rpm1–3* knockout mutant, and two independent *RPM1-DN* transformants (*RPM1-DN1* and *RPM1-DN2*), using an electrolyte leakage assay (Mackey et al., 2003). As expected, cell death measured as conductance increased in Col-0 already after 3 hr (Figure 1A). However, this increase was suppressed in *RPM1-DN1* and *RPM1-DN2* plants to the same extent as in *rpm1–3* (Figure 1A). We also tested resistance responses in 4-week-old, short-day-grown rosette leaves syringe infiltrated with *Pst* DC3000 (AvrRpm1), by measuring bacterial growth at 0 and 3 days. After 3 days, bacterial growth was almost 100-fold higher in *RPM1-DN1*, *RPM1-DN2*, and *rpm1–3* compared to Col-0 (Figure 1B). Moreover, we did not observe any difference in growth of virulent *Pst* DC3000 among Col-0, *rpm1–3* mutants, and plants expressing *RPM1-DN* (Figure 1C). Thus, expression of *RPM1-DN* in wild-type plants compromises the function of RPM1.

We then tested the specificity of this dominant suppression by examining if resistance to bacteria expressing AvrRps4 and AvrRpt2 was affected by the expression of *RPM1-DN*. AvrRps4 is recognized by the TIR-NLR pairs RPS4/RRS1 and RPS4B/RRS1B (Narusaka et al., 2009; Saucet et al., 2015), whereas resistance against AvrRpt2 is conferred by the CC-NLR RPS2 (Tsuda et al., 2013). This revealed that two *RPM1-DN* lines supported similar levels of growth of *Pst* DC3000 (AvrRps4) as Col-0 and *rpm1–3*, while the susceptible control *eds1–2* supported significantly higher growth (Figure 2A). Similarly, expression of *RPM1-DN* did not interfere with recognition of AvrRpt2, as the *RPM1-DN* lines did not support more bacterial growth than Col-0 (Figure 2B). As expected, the susceptible control *ndr1* supported significantly higher bacterial growth than the other genotypes (Figure 2B). Thus, plants expressing dominant-negative versions of *RPM1* are indistinguishable from *rpm1–3* mutants and the function of other NLRs is unaffected. Lastly, to confirm that mutations in specific NLRs can suppress single autoimmune mutants, we mutated the P loop in *SUMM2.* Loss-of-function mutations in the de-capping activator *PAT1* (*PROTEIN ASSOCIATED WITH TOPOISOMERASE II NUMBER 1*) lead to SUMM2-dependent autoimmunity, including dwarfism and elevated levels of the defense marker *PATHOGENESIS RELATED* 1 (*PR1*) transcripts (Roux et al., 2015). Similar to *pat1 summ2* double homozygotes, expression of *SUMM2-DN* in *pat1* suppressed dwarfism, enhanced resistance, and elevated *PR1* transcript levels (Figure S1). Thus, as in *pat1 summ2* plants, autoimmunity is suppressed in *pat1* mutants expressing *SUMM2-DN*.

Introducing a P Loop Mutation in Multiple *Arabidopsis* NLRs

The proof of concept with DN mutant forms of *RPM1* and *SUMM2* prompted us to introduce such mutations into an additional 106 *Arabidopsis* NLRs (Table S1). These NLRs were used because they were readily cloned/mutated and because they

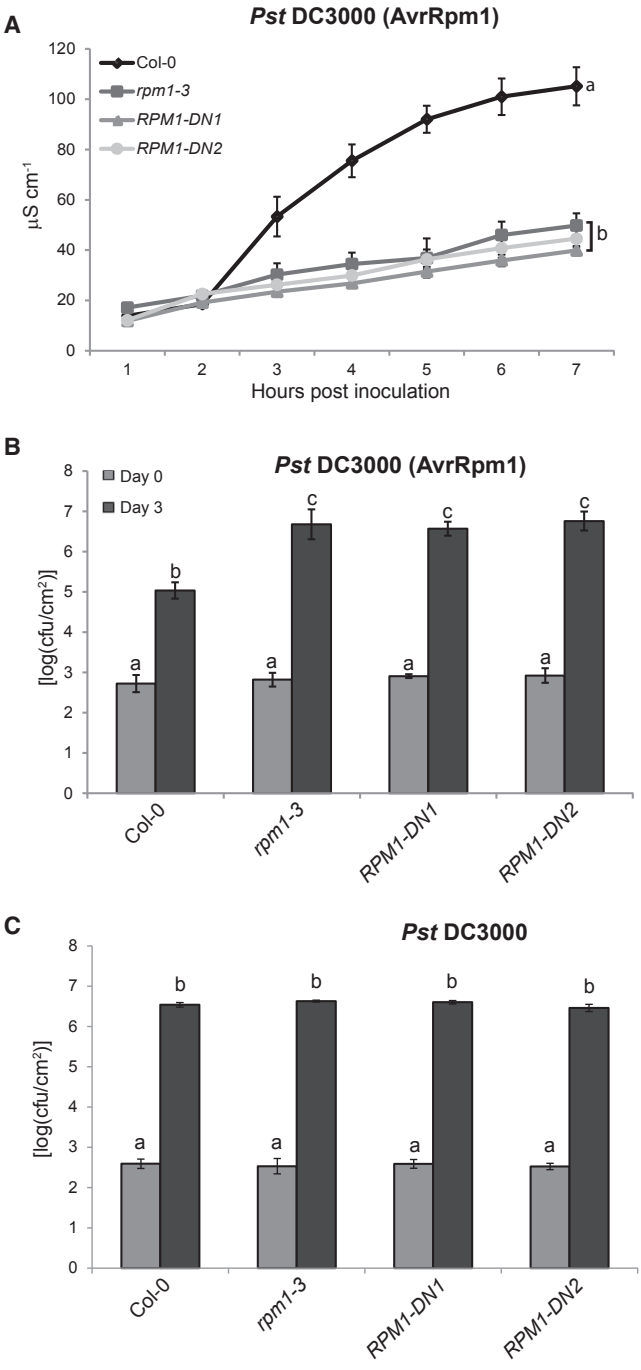

Figure 1. Expression of *RPM1-DN* Compromises RPM1 Function and Attenuates Resistance

(A) AvrRpm1-dependent cell death is inhibited by *RPM1-DN* expression. Ion leakage assay after inoculation of *Pst* DC3000 (AvrRpm1) into Col-0, *rpm1–3*, or two transgenic lines overexpressing *RPM1-DN* (line *RPM1-DN1* and *2*) is shown. Error bars represent ±SD. Groups with statistically different means are indicated by different letters.

(B and C) Col-0 resistance to *Pst* DC3000 (AvrRpm1, B) is compromised by *RPM1-DN* expression. No effect is seen in resistance to *Pst* DC3000 carrying an empty vector (C). Growth of *Pst* DC3000 (AvrRpm1 or empty vector) at days 0 (gray) and 3 (black) as log10-transformed colony-forming units per square centimeter leaf tissue (CFU/cm^2) is shown. Error bars represent ±SD (n = 4). Means not sharing the same letter are significantly different.

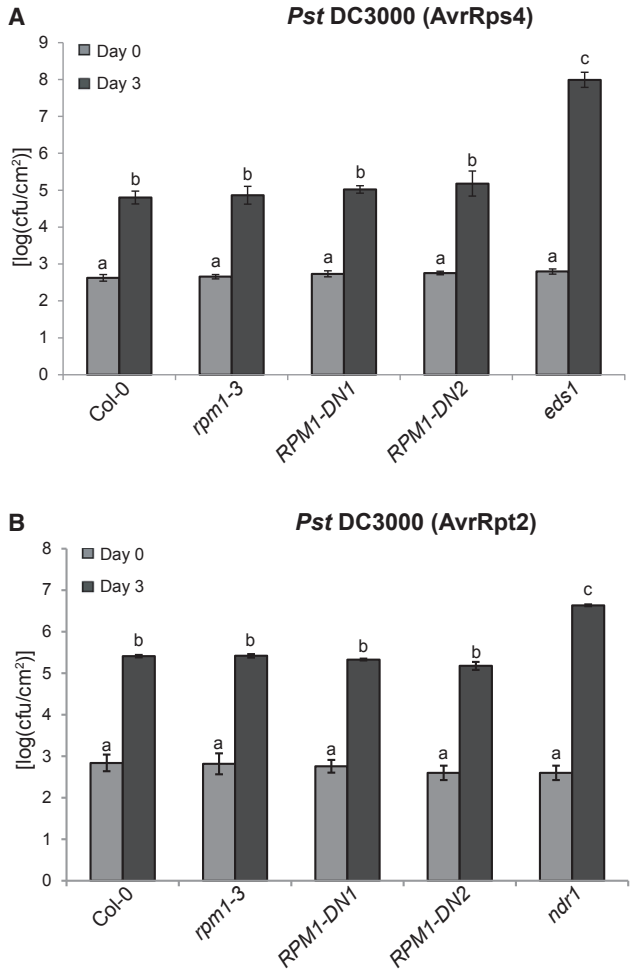

Figure 2. *RPM1-DN* Expression Specifically Inhibits RPM1 Function and Does Not Compromise Resistance to AvrRps4 or AvrRpt2

(A and B) Wild-type resistance to *Pst* DC3000 (AvrRps4 and AvrRpt2) is retained in transgenic *RPM1-DN* plants. Col-0, *rpm1–3*, *RPM1-DN1*, *RPM1-DN2*, and *eds1-2* or *ndr1-1* were inoculated with *Pst* DC3000 (AvrRps4, A, and AvrRpt2, B). Bacterial growth was measured on days 0 (gray) and 3 (black). Mean ± SD (n = 4) is shown and means not sharing the same letter are significantly different.

encode typical TIR- (72 genes) or CC-NLRs (34 genes) without truncations or additional domains. With *RPM1* and *SUMM2*, this allele collection represents 89% (73/82) of *Arabidopsis* TIR-NLRs and 73% (35/48) of CC-NLRs (Meyers et al., 2003). More specifically, the conserved P loop motif GXXXX**GK**T(T/S) in these genes was mutated to GXXXX**AA**T(T/S) using mismatch primers and a multi-fragment USER cloning approach (Geu-Flores et al., 2007). Sequenced clones were introduced into *Agrobacterium* GV3101 and then transformed into wild-type plants and a collection of autoimmune mutants, including *camta3*. Independent T1 plants (T2 seeds) were collected after BASTA selection and screened for suppression of stunted growth, chlorosis, or early flowering phenotypes exhibited by the autoimmune mutants. In a screen of ~60 NLR-DN-expressing lines, we identified one line exhibiting suppression of the *camta3* phenotype (Figure 3A). We named this line, which

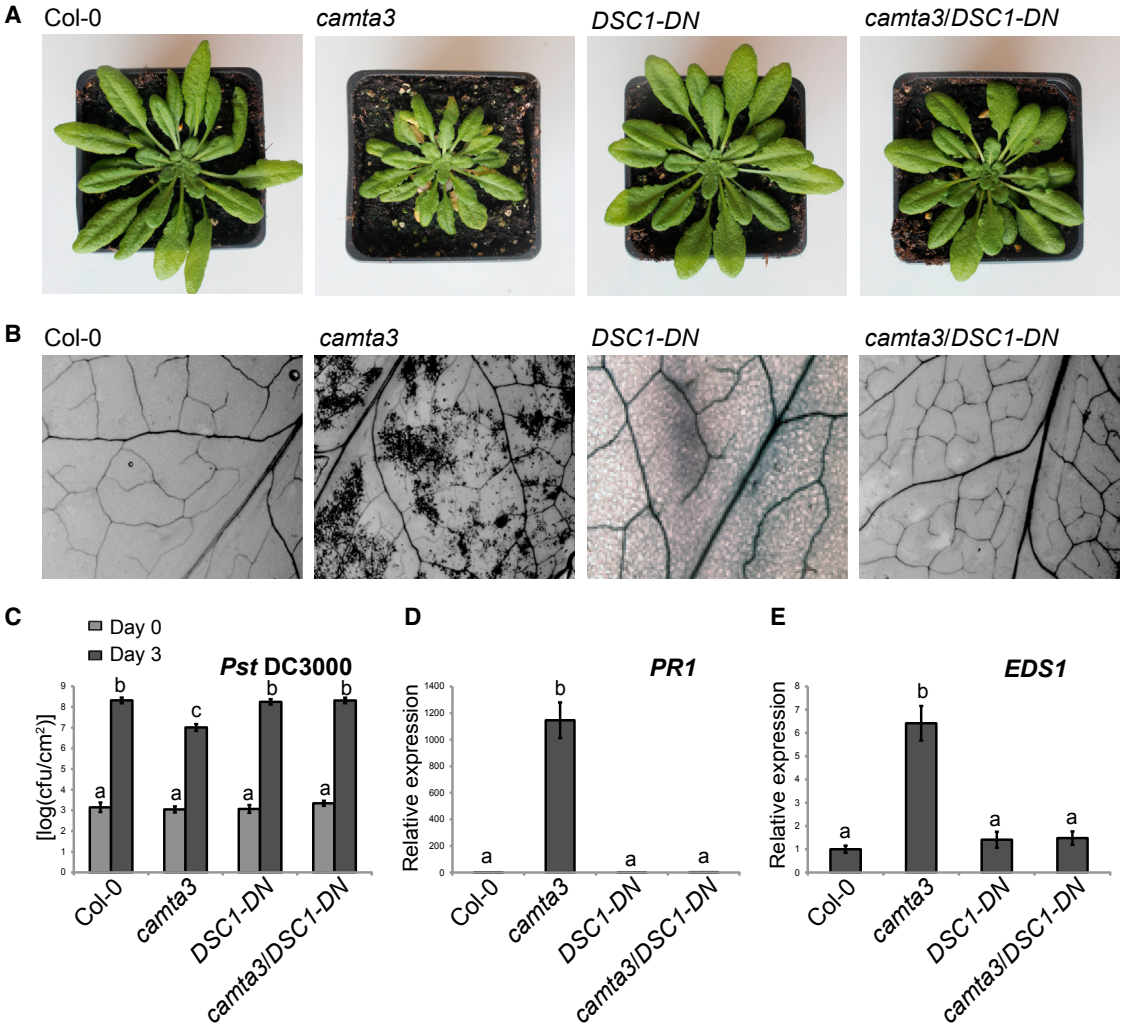

Figure 3. *DSC1-DN* Suppresses *camta3* Autoimmune Phenotypes

(A) *camta3* growth and chlorosis phenotypes are rescued by the expression of *DSC1-DN*. Pictures are representative for several individual lines.

(B) *camta3* microscopic lesions are suppressed by the expression of *DSC1-DN*. Trypan blue-stained leaves of Col-0, *camta3*, *DSC1-DN*, and *camta3 DSC1-DN* (one representative of several individual lines) are shown.

(C) Expression of *DSC1-DN* suppresses resistance in *camta3* mutants. Plants were inoculated with *Pst* DC3000 and colony-forming units per square centimeter are plotted for days 0 (gray) and 3 (black). Error bars represent ±SD (n = 4).

(D and E) *PR1* and *EDS1* mRNA levels are elevated in *camta3* mutants, but they are reduced to wild-type levels in *camta3* expressing *DSC1-DN*. The mRNA levels for *PR1* (D) and *EDS1* (E) are shown. Error bars represent mean ± SD (n = 3). Means not sharing the same letter are significantly different.

expresses the DN form of the NLR encoded by *At4g12010*, *DSC1-DN* for *DOMINANT SUPRESSOR OF camta3 NUMBER 1-DOMINANT NEGATIVE*. *DSC1* encodes a typical TIR-NLR proposed to be part of an NLR pair together with the TIR-NLR *At4g12020* (Narusaka et al., 2009). This head-to-head pair may share a small promoter region of 273 bp and both genes are lowly expressed (AtGenExpress). However, Meyers et al. (2003) found that DSC1 is one of only 38 NLRs for which mRNA expression levels are affected by SA or flg22, while *At4g12020* is not. Although *At4g12020* is the closest homolog of DSC1, it contains WRKY and MAPx kinase domains and was, therefore, not included in our NLR-DN collection.

There are six CAMTA proteins in *Arabidopsis*, and null alleles of *CAMTA1* or *CAMTA2* in *camta3* mutants enhance the latter's dwarfism and chlorosis (Kim et al., 2013). However, expression of *DSC1-DN* in *camta1 camta3* double mutants did not suppress this growth defect. This indicates that *DSC1-DN* suppression is specific to *CAMTA3* (Figure S2).

NLR-Dependent Autoimmunity in *camta3*

T3 lines homozygous for *DSC1-DN* were examined for suppression in more detail. The 6-week-old *camta3* mutants grown in short days exhibited stunted growth, necrotic lesions in older leaves (Figure 3A), and clusters of dead mesophyll cells (Figure 3B) (Du et al., 2009). In contrast, *camta3 DSC1-DN* appeared wild-type (Figures 3A and 3B). Expression of *DSC1-DN* in Col-0 did not affect its wild-type growth and did not induce cell death (Figures 3A and 3B).

The *camta3* mutants also exhibit increased resistance toward virulent *Pst* DC3000 (Galon et al., 2008). To evaluate if this trait was also abrogated by expression of *DSC1-DN*, we syringe inoculated 5-week-old plants with *Pst* DC3000 and measured bacterial growth after 3 days. While bacterial growth in *camta3* mutants was significantly lower than in Col-0, bacterial growth was restored to wild-type levels in *camta3 DSC1-DN* (Figure 3C). Importantly, expression of *DSC1-DN* in Col-0 did not affect susceptibility (Figure 3C).

The *camta3* mutants constitutively express defense genes, including *PR1* (Du et al., 2009). However, *PR1* mRNA levels were restored to Col-0 levels in *camta3 DSC1-DN* lines, and the expression of *DSC1-DN* in Col-0 did not affect *PR1* mRNA levels (Figure 3D).

Since CAMTA3 was found to bind the *EDS1* promoter and was reported to be a negative regulator of *EDS1* expression, elevated levels of *EDS1* and other CAMTA3-regulated transcripts were thought to cause autoimmunity in *camta3* (Du et al., 2009). While autoimmunity in *camta3* mutants may be suppressed by *DSC1-DN*, expression of *EDS1* should remain elevated in *camta3 DSC1-DN*. In agreement with previous reports, we found that *EDS1* mRNA levels were significantly higher in 5-week-old *camta3* compared to Col-0 plants (Figure 3E). However, the levels of *EDS1* transcripts in *camta3 DSC1-DN* were not significantly different from those in Col-0 or *DSC1-DN* single mutants (Figure 3E). These results indicate that autoimmunity in *camta3* mutants is triggered by DSC1 and not by the loss of negative regulation of *EDS1* and other regulatory transcripts.

CAMTA3 Interacts with DSC1 and Inhibits DSC1-Triggered HR in *N. benthamiana*

To further investigate the relationship between DSC1 and CAMTA3, we expressed them in *N. benthamiana* as transient overexpression of NLRs can trigger HR cell death in this system (Césari et al., 2014). In line with this, expression of *DSC1* alone triggered strong and rapid HR-like cell death (Figure 4A). This DSC1-triggered HR was suppressed by co-expression with *CAMTA3* (Figure 4A), while co-expression of *CAMTA1* or *CAMTA2* had no influence on DSC1-triggered HR (Figure 4A). Expression of the three *CAMTA*s alone did not induce a reaction. DSC1, therefore, acts as an HR trigger specifically in the absence of CAMTA3.

The above results suggest that DSC1 and CAMTA3 represent a guard/guardee pair. We therefore speculated that DSC1 and CAMTA3 may be found together in subcellular complexes. To assess this, we examined the localization of CAMTA3 fused to CFP (Figure S3A) and DSC1 fused to yellow flourescent protein (YFP) (Figure S3B). Since both showed cytoplasmic and nuclear localization when transiently expressed in *N. benthamiana*, we tested their interaction in vivo by Förster resonance energy transfer acceptor bleaching (FRET-AB). Using CFP_CAMTA as donor and YFP_DSC1 as acceptor, we observed a clear increase in donor fluorescence (FRET efficiency) after photobleaching of YFP (Figure 4B). The same FRET efficiency was not seen with donor/acceptor pairs of CFP_CAMTA and YFP_SUMM2 or CFP_MPK4 and YFP_DSC1, included as negative controls (Figure 4C). To confirm the positive FRET, we transiently expressed HA_DSC1 with CAMTA3_CFP or GFP_MYC in *N. benthamiana* and immunoprecipitated DSC1 with HA-trap beads. Only CAMTA3_CFP was detected in HA_DSC1 precipitates (Figure 4D), confirming that DSC1 and CAMTA3 can exist in complexes in planta.

Autoimmunity in *camta3* Depends on Two NLRs

To further probe connections between DSC1 and CAMTA3, we generated *camta3 dsc1* double loss-of-function mutants. Surprisingly, these double mutants appeared indistinguishable from *camta3* single mutants (Figure 5A), and, upon inoculation with *Pst* DC3000, they showed *camta3*-like enhanced resistance (Figure 5B). In addition, like *camta3*, *camta3 dsc1* had elevated levels of *PR1* and *EDS1* expression (Figures 5C and 5D). This suggests that *DSC1-DN* interferes with more than just DSC1 function. As two or more NLRs may guard the same guardee (Belkhadir et al., 2004; Eitas et al., 2008) and as NLRs may dimerize (Eitas and Dangl, 2010; Narusaka et al., 2009, 2013), we speculated that DSC1 might function together with another NLR. If so, DSC1-*DN* might poison their cooperativity while the absence of DSC1 in the *dsc1* mutant would not. We therefore screened our remaining NLR-DN alleles for suppression of *camta3* autoimmunity, and we found an NLR-DN allele of *At5g18370*, here called *DSC2-DN*, whose expression also fully suppressed the *camta3* phenotypes (Figure 6A). The closest *DSC2* homolog (*At5g18350*), separated from it by ~10 kb encoding both a TIR-NLR (*At5g18360*) and another gene (*At5g18362*), was included in the NLR-DN screen, but it did not exhibit suppression of *camta3*.

As for *DSC1-DN*, expression of *DSC2-DN* in *camta3* abrogated resistance to *Pst* DC3000 (Figure 6B) and restored *PR1* expression almost to wild-type levels (Figure 6C). Expression of *DSC2-DN* in Col-0 did not affect resistance or *PR1* expression levels. Importantly *EDS1* mRNA levels in *camta3 DSC2-DN* were similar to those in Col-0 and *DSC2-DN* (Figure 6D). We also found that, as for *DSC1*, transient expression of *DSC2* in *N. benthamiana* triggered HR-like cell death, which was suppressed by co-expression with *CAMTA3* (Figure 6E). This again indicates that autoimmunity in *camta3* mutants is triggered by NLRs and is not due to the loss of CAMTA3 as a negative regulator of *EDS1*.

We generated *camta3 dsc2* double mutants to further examine the connection between CAMTA3 and DSC2. Unlike *camta3*, *camta3 dsc2* did not exhibit dwarfism, but leaf development was not restored to wild-type (Figure S4A). The *camta3 dsc2* mutants also had only partial suppression of resistance toward *Pst* DC3000 (Figure S4B), and they showed higher expression of *PR1* and *EDS1* compared to wild-type (Figures S4C and S4D).

Since *camta3 dsc1* showed no suppression and *camta3 dsc2* showed only partial suppression of the *camta3* autoimmune phenotypes, we generated triple *camta3 dsc1 dsc2* mutants. These triple mutants appeared wild-type and developed like Col-0 (Figure 7A), while *camta3* growth defects were restored in the triple mutant complemented with genomic clones of either *DSC1* or *DSC2* (Figure S5). Although the triple mutants did not develop visible autoimmune phenotypes, it was possible that they retained increased pathogen resistance. To test this, we inoculated leaves of Col-0, *camta3*, and *camta3 dsc1 dsc2* with *Pst* DC3000. This demonstrated that *camta3 dsc1 dsc2* resistance

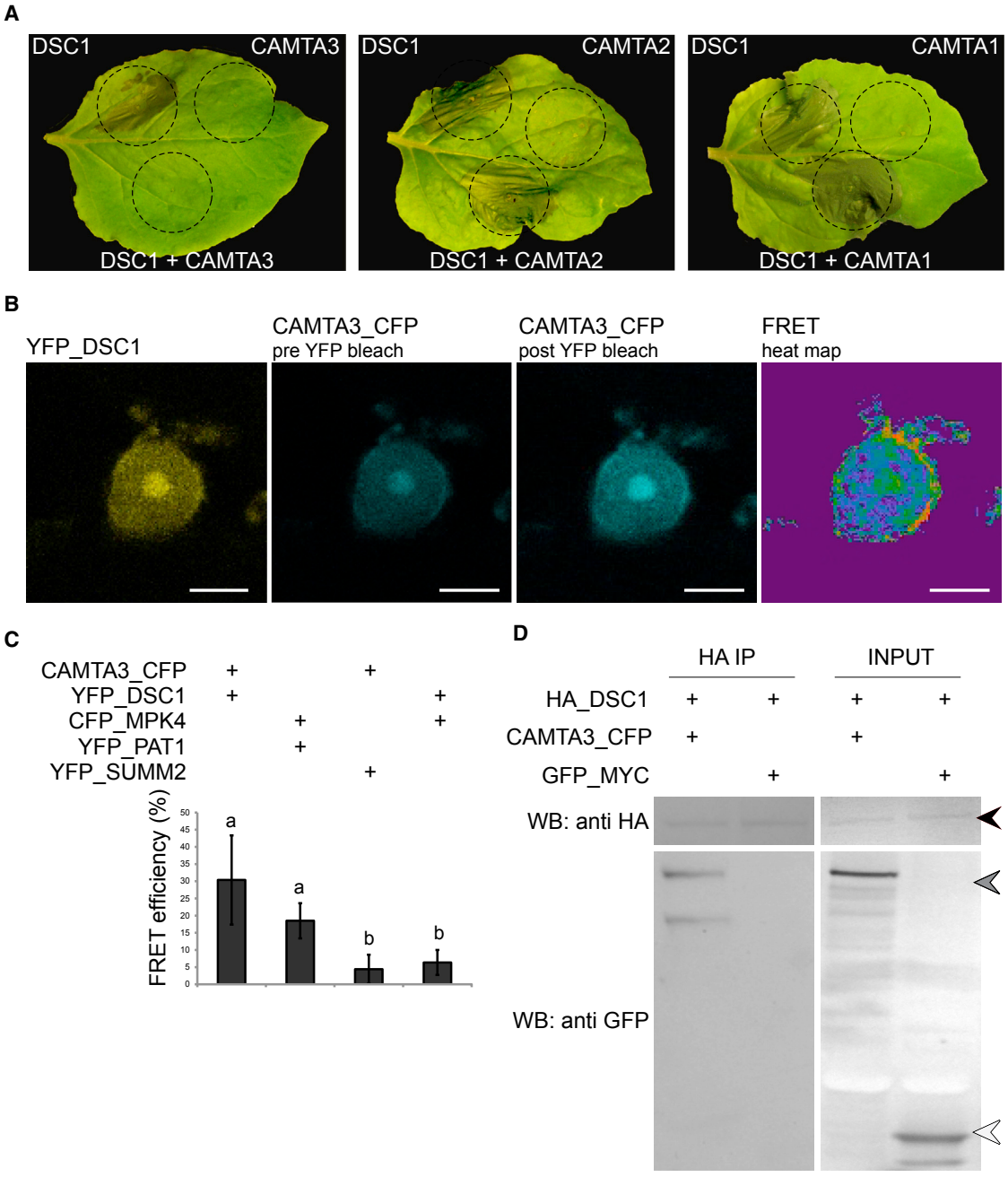

Figure 4. CAMTA3 Is Associated with DSC1 in *N. benthamiana*

(A) Expression of *CAMTA3* rescues DSC1-induced cell death in *N. benthamiana*. Inoculation with *Agrobacterium* expressing *DSC1* resulted in HR induction. Co-inoculation with *CAMTA3* inhibited this DSC1-induced cell death. Co-inoculation with *CAMTA1* or *CAMTA2* failed to inhibit the induction of HR. Dashed lines mark infiltrated areas.

(B and C) Detection of in vivo interaction between CAMTA3 and DSC1 by FRET in *N. benthamiana*. CFP_CAMTA3 and YFP_DSC1 were co-expressed in *N. benthamiana* and analyzed for FRET-AB. CFP_MPK4 and YFP_PAT1 were included as positive controls. Negative controls are CFP_CAMTA with YFP_SUMM2 and CFP_MPK4 with YFP_DSC1. Error bars represent ± SD (n = 4). Means not sharing the same letter are significantly different. See also Figure S3.

(D) CAMTA3 is associated with DSC1 in *N. benthamiana*. HA_DSC1 and CAMTA3_CFP or GFP_MYC were co-expressed in *N. benthamiana* and tissue was harvested at 24 hpi. Immunoblots of input and anti-HA immunoprecipitates (IPs) probed with anti-HA and anti-GFP antibodies are shown. Left panel, anti-HA IP; right panel, input; black arrow, HA_DSC1; gray arrow, CAMTA3_CFP; white arrow, GFP_MYC.

was restored to wild-type levels (Figure 7B). While increased resistance was seen in *camta3* and in *camta3 dsc1* and *camta3 dsc2* 3 days post-inoculation (Figures 5B and S4B), bacterial growth in *camta3 dsc1 dsc2* reached the same levels seen in Col-0 and in *camta3 DSC1-DN* and *camta3 DSC2-DN* (Figures 7B, 3B, and 6B). In addition, *PR1* levels were restored to

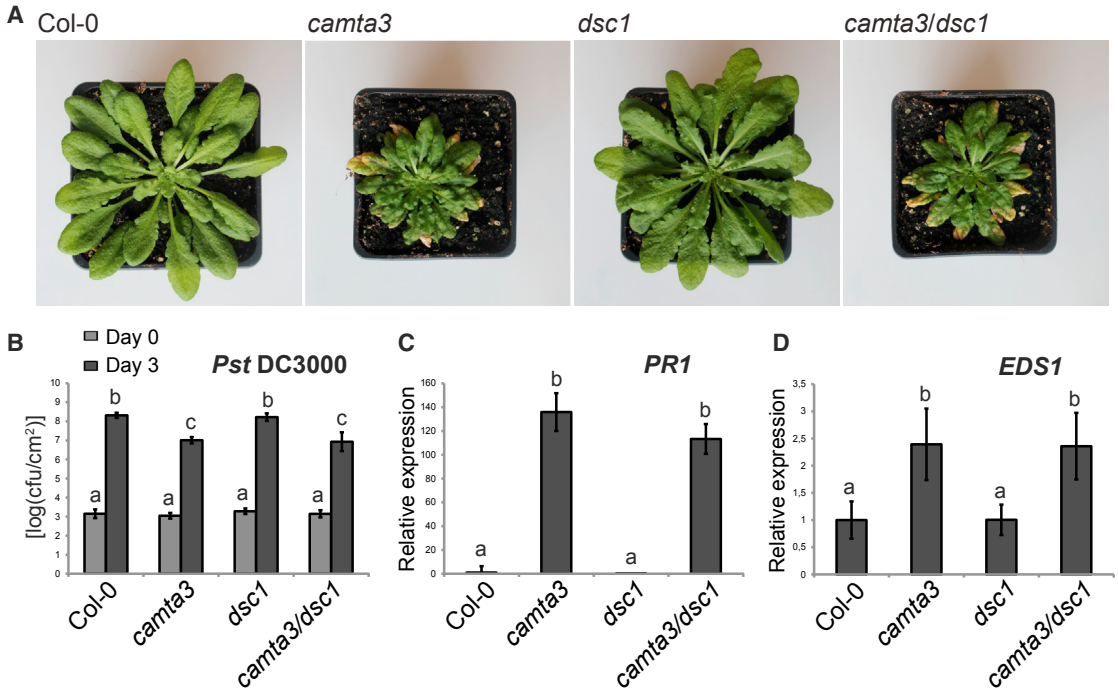

Figure 5. A T-DNA Insertion in *DSC1* Does Not Suppress the *camta3* Autoimmune Phenotypes

(A) The phenotypes of *camta3* and *camta3 dsc1* are indistinguishable. Morphological phenotypes of Col-0, *camta3*, *dsc1*, and *camta3 dsc1* double mutant are shown.

(B) Resistance is similar in *camta3 dsc1* double and *camta3* mutants. Plants were infiltrated with *Pst* DC3000 and colony-forming units per square centimeter plotted for days 0 (gray bars) and 3 (black). Error bars represent ±SD (n = 4).

(C and D) *PR1* and *EDS1* mRNA levels in the *camta3 dsc1* double mutant are the same as in *camta3*. Relative *PR1* (C) and *EDS1* (D) mRNA levels in *camta3*, *dsc1*, and *camta3 dsc1* mutants determined by qRT-PCR are shown. Error bars represent ±SD (n = 3). Bars with different letters are significantly different.

wild-type levels in the *camta3 dsc1 dsc2* triple mutant (Figure 7C), in contrast to the higher levels in *camta3 dsc1* and *camta3 dsc2* (Figures 5C and S4C). Furthermore, *EDS1* mRNA levels in *camta3 dsc1 dsc2* plants were similar to those in Col-0 (Figure 7D).

In summary, *DSC1* and *DSC2* contribute to autoimmunity in *camta3*. Although they seem to operate independently, the fact that the dominant-negative version of either one influences the other suggests that DSC1 and DSC2 interact directly or indirectly. To test this, we transiently expressed HA_DSC1 with DSC2_YFP, YFP_DSC2, or GFP-MYC in *N. benthamiana*, and we immunoprecipitated DSC2 with GFP-trap beads. As a specificity control, we also expressed DSC2-YFP, YFP-DSC2, and GFP-MYC with HA-RPS4 (Zhang et al., 2004), as DCS1 and RPS4 share 61% amino acid identity. HA_DSC1 could only be detected in DSC2 precipitates and not in GFP_MYC precipitates (Figure 7E). In contrast, RPS4 was not detected in the DSC2_YFP precipitates, although a faint RPS4 band was observed in the YFP_DSC2 precipitates when expressed at similar levels to DSC1 at 24 hr post-inoculation (hpi) (Figure 7E). In line with this, expression of *RPS4* alone triggered strong and rapid HR-like cell death only a few days after infiltration, which was not suppressed by co-expression with *CAMTA3* (Figure 7F). These data show that DSC2 preferentially co-immunoprecipitates with DSC1, indicating that they may be found in complexes in planta.

DISCUSSION

Arabidopsis autoimmune mutants have been intensively studied for more than 20 years (Dietrich et al., 1994; Greenberg and Ausubel, 1993; Greenberg et al., 1994). Many reports link autoimmune phenotypes to NLR-signaling pathways and recently also directly to *NLR* genes (Bonardi et al., 2011; Bruggeman et al., 2015; Palma et al., 2010; Roux et al., 2015; Zhang et al., 2012). We hypothesized that numerous phenotypes related to autoimmunity may be caused by NLR activation. This implies that specific mutations in host plant guardees mimic pathogen effector activities and trigger the corresponding NLR guards.

To examine this possibility, we introduced specific mutations into the P loops of a large collection of NLRs. This approach was supported by (1) the conservation of the P loop in the STAND and closely related NLR families (Leipe et al., 2004); (2) the dominant-negative effects of such mutations on the *Arabidopsis* LAZ5 and tobacco N NLRs (Dinesh-Kumar et al., 2000; Mestre and Baulcombe, 2006; Palma et al., 2010); and (3) the possibility that numerous NLRs form dimers or directly or indirectly associate in complexes (Mestre and Baulcombe, 2006), leading to dominant-negative subunit poisoning.

As proof of concept, we compromised the function of RPM1 by expressing its dominant-negative version, and we showed that this suppression was specific and did not affect general NLR function (Figures 1 and 2). Abolition of RPM1 function by

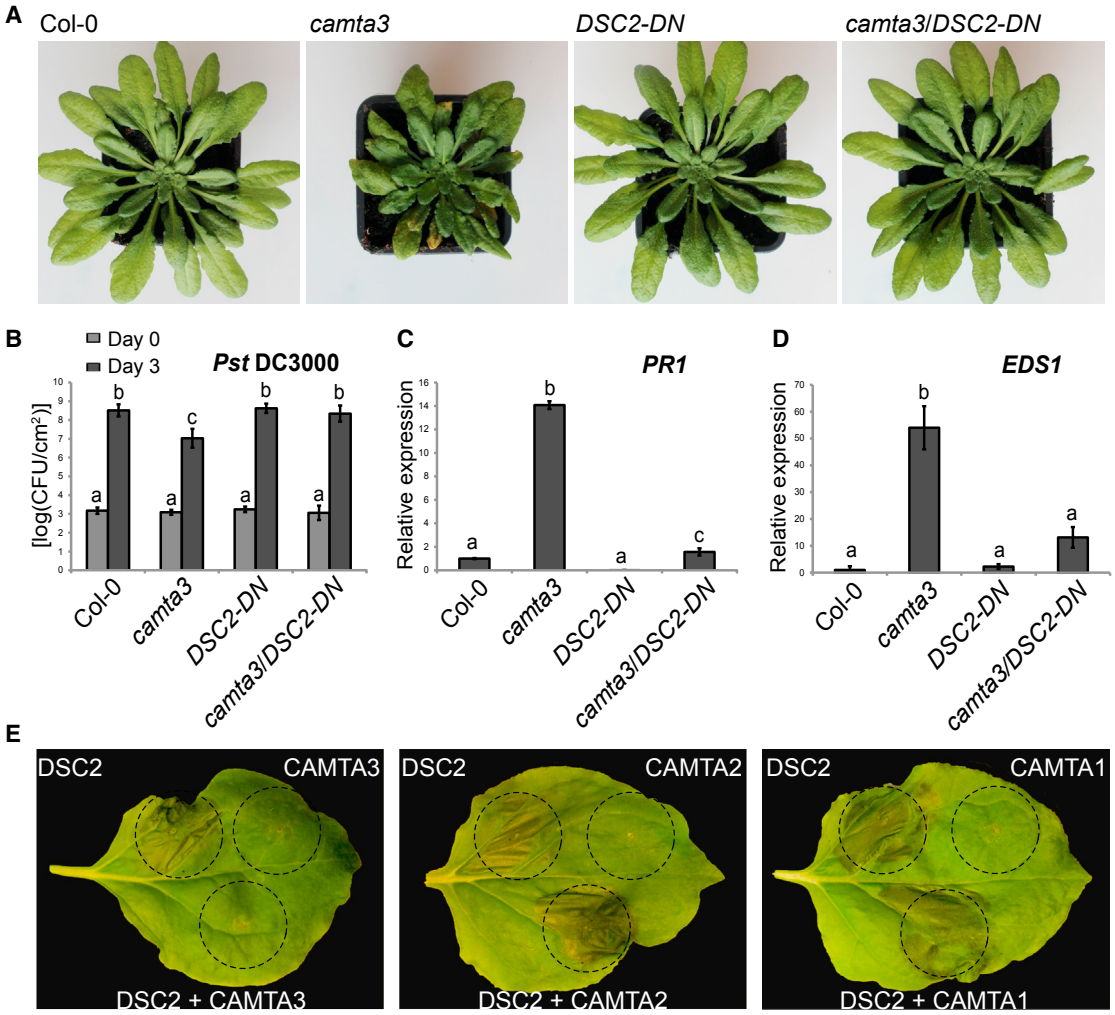

Figure 6. *DSC2-DN* Transgene Suppresses the *camta3* Autoimmune Phenotypes

(A) *camta3* growth and chlorosis phenotypes are rescued by the expression of *DSC2-DN*. Pictures are representative for several individual lines.

(B) Expression of *DSC2-DN* suppresses resistance in *camta3* mutants. Plants were syringe inoculated with *Pst* DC3000 and colony-forming units per square centimeter counted on days 0 (gray bars) and 3 (black). Error bars represent ±SD (n = 4). Bars with different letters are significantly different.

(C) *PR1* mRNA levels are reduced to almost wild-type levels in *camta3* mutants expressing *DSC2-DN*. *PR1* mRNA expression levels are shown. Error bars represent ±SD (n = 3). Letters indicate statistical significance.

(D) *EDS1* mRNA levels are elevated in *camta3* mutants, but they are similar to Col-0 levels in *camta3 DSC2-DN*. The mRNA levels for *EDS1* are shown. Error bars represent mean ± SD (n = 3). Means not sharing the same letter are significantly different.

(E) Expression of *CAMTA3* rescues *DSC2*-induced cell death in *N. benthamiana*. Inoculation with *Agrobacterium* expressing *DSC2* results in the induction of HR. Co-inoculation with *CAMTA3* inhibits the DSC2-induced cell death. Co-inoculation with *CAMTA1* or *CAMTA2* failed to inhibit HR induction. Areas of infiltration are marked by dashed lines.

P loop mutation was shown previously (Chung et al., 2011; Tornero et al., 2002), but not the dominant-negative effect described here. In addition, we found that expression of *SUMM2-DN* suppressed autoimmunity in *pat1* mutants (Figure S1). Thus, NLR-DN alleles can be made via simple P loop mutagenesis.

We then conducted a screen to identify other NLR-DN alleles that suppress the autoimmune phenotype of the *camta3* mutant (Galon et al., 2008). This screen identified *DSC1-DN* and *DSC2-DN*. CAMTA3 was described as a negative regulator of immunity due to the ectopic accumulation of defense-related transcripts, including *EDS1* in *camta3* mutants, and to the suppression of *camta3* phenotypes in *camta3 eds1* double mutants (Du et al., 2009). However, *EDS1* is ectopically expressed in many autoimmune mutants, and *EDS1* mutations suppress autoimmunity in many of them (Bruggeman et al., 2015; Rodriguez et al., 2016). We show here that *EDS1* mRNA levels are similar to those in wild-type when *DSC1-DN* or *DSC2-DN* is expressed in *camta3* (Figures 3E and 6D). Importantly, the increased resistance to virulent *Pst* DC3000 in *camta3* was also reduced to wild-type (WT) levels in *camta3* expressing either *DSC1-DN* or *DSC2-DN* (Figures 3C and 6B). These findings do not support a function for CAMTA3 as a negative

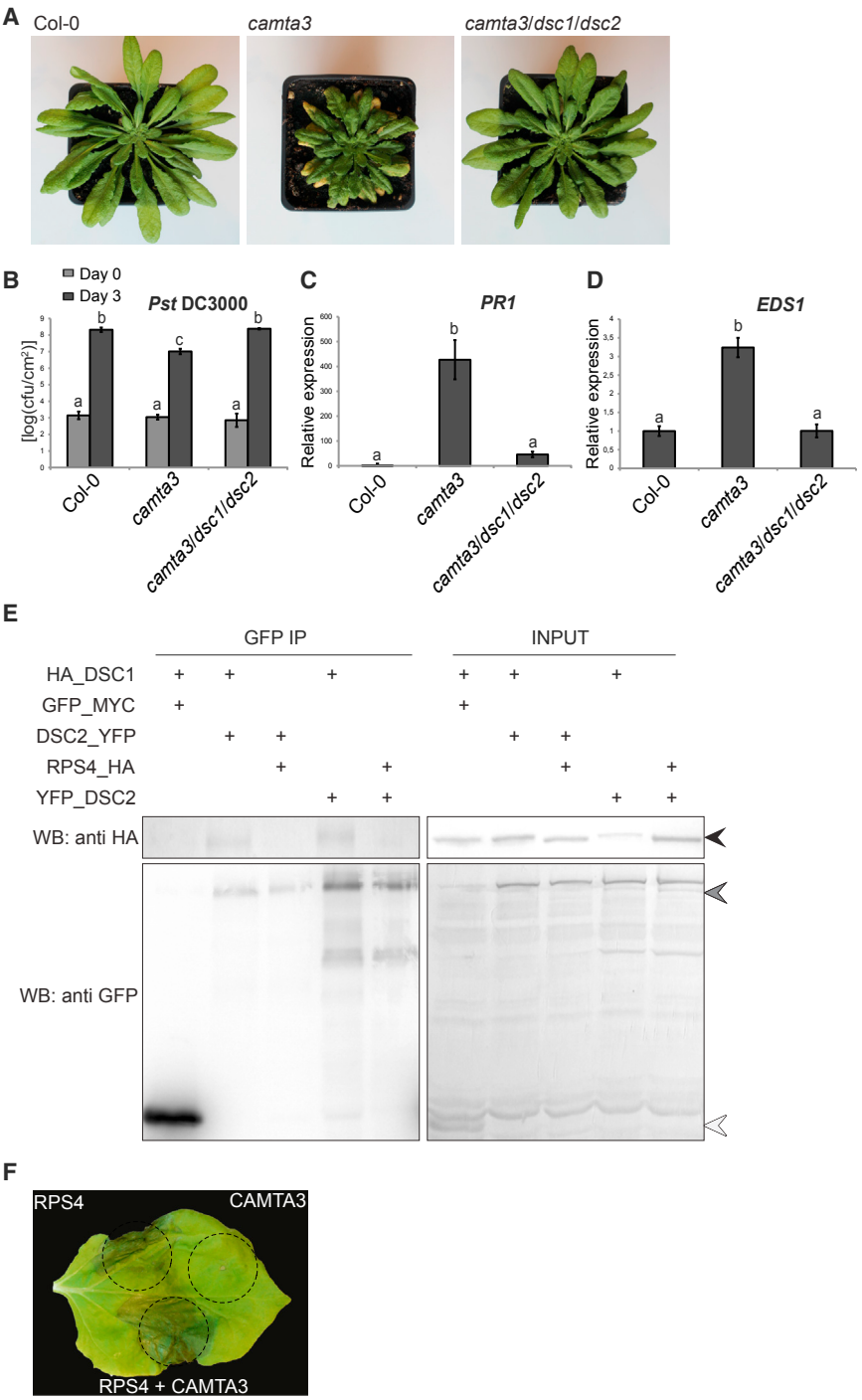

Figure 7. *camta3 dsc1 dsc2* Triple Mutants Rescue All *camta3* Phenotypes

(A) *camta3 dsc1 dsc2* triple mutants develop like wild-type Col-0. Representative images of several individual lines are shown. See also Figures 5, S4, and S5.

(B) *camta3* resistance to *Pst* DC3000 is suppressed in the triple *camta3 dsc1 dsc2* mutant. Colony-forming units per square centimeter were counted at days 0 (gray bars) and 3 (black). Error bars represent mean ± SD (n = 4). Bars with different letters are significantly different.

(C and D) *PR1* and *EDS1* mRNA levels in *camta3* are completely abolished in the *camta3 dsc1 dsc2* triple mutant. The mRNA levels for *PR1* (C) and *EDS1* (D) are shown relative to wild-type Col-0. Error bars represent mean ± SD (n = 3). Means not sharing the same letter are significantly different.

(E) DSC2 is associated with DSC1 in *N. benthamiana*. DSC1_HA + DSC2_YFP, YFP_DSC2, or GFP_MYC and RPS4_HA + DSC2_YFP or YFP_DSC2 were co-expressed in *N. benthamiana*. Left panel, anti-HA IP; right panel, input; black arrow, HA_DSC1/RPS4_HA; gray arrow, DSC2_YFP/YFP_DSC2; white arrow, GFP_MYC.

(F) RPS4-induced cell death in *N. benthamiana* is not rescued by expression of *CAMTA3*. Inoculation of *N. benthamiana* leaves with *RPS4* resulted in HR induction. Co-inoculation with *CAMTA3* did not affect RPS4-induced cell death. Areas of infiltration are marked by dashed lines.

regulator of either *EDS1* expression or resistance to the pathogen tested.

Nonetheless, Du et al. (2009) provided other evidence that CAMTA3 negatively regulates *EDS1* expression. First, CAMTA3 recognized an *EDS1* promoter element that was responsible for suppression of a reporter gene driven by the *EDS1* promoter. Second, chromatin immunoprecipitation in protoplasts with transiently overexpressed, YFP-tagged CAMTA3 showed enrichment of *EDS1* promoter elements, confirming that CAMTA3 can bind *EDS1* promoter elements (Du et al., 2009). Third, plants that overexpress *CAMTA3* exhibit increased susceptibility to virulent *Pst* DC3000 (Jing et al., 2011). Nonetheless, these and other data (Du et al., 2009; Nie et al., 2012) do not provide direct evidence for inhibition of transcription by CAMTA3. More recently, the rapid stress response element (RSRE), characterized in promoters that rapidly respond to stresses including flg22 (Walley et al., 2007), was identified as a core CAMTA3-binding element. In addition, CAMTA3 could transiently activate the expression of a RSRE:LUC reporter (Benn et al., 2014), and a *camta3* mutant exhibited reduced RSRE:LUC activity (Bjornson et al., 2014). Similarly, a general stress response and RSRE induction is CAMTA3 dependent (Benn et al., 2016). These findings indicate that CAMTA3 is a positive regulator of early stress responses. While CAMTA3 may thus possess both positive and negative regulatory activities, our data indicate that autoimmunity in *camta3* is NLR triggered.

Our results are consistent with a model in which DSC1 and DSC2 guard CAMTA3 and/or a complex or pathway in which CAMTA3 functions. Importantly, we show that CAMTA3 may exist in complexes with DSC1 in planta (Figures 4B–4D).

Moreover, both DSC1 and DSC2 can trigger the HR when expressed in *N. benthamiana*, but co-expression of *CAMTA3* prevents this (Figures 4A and 6E). Thus, these two NLRs appear inactive in the presence of CAMTA3 but are activated in its absence. This is analogous to immunity triggered by RPS2 upon effector-mediated degradation of the host guardee RIN4 (Axtell and Staskawicz, 2003; Mackey et al., 2003).

Interestingly, *camta3* autoimmune phenotypes were not suppressed in *camta3 dsc1* or *camta3 dsc2* double loss-of-function mutants. This may be explained if both DSC1 and DSC2 can be triggered in the absence of CAMTA3. In line with this, autoimmunity was completely suppressed in *camta3 dsc1 dsc2* triple loss-of-function mutants. Thus, autoimmunity in *camta3* can be triggered by both NLRs, and the function of both must be abrogated to prevent autoimmunity.

These findings and the co-immunoprecipitation of DSC1 with DSC2 in *N. benthamiana* suggest that they interact. Such interactions probably do not only involve direct heterodimerization under natural conditions, as such heterodimer formation would be disrupted in their single *dsc1* or *dsc2* loss-of-function mutants, leading to the suppression of *camta3* mutant phenotypes. Alternatively, the DSC1 and DSC2 co-precipitation is consistent with indirect associations via complexes with CAMTA3 or an *N. benthamiana* ortholog. In a simple model, if activation of such complexes was dependent on either or both DSC1 and DSC2, then activation might be compromised by overexpression of the DN form of either NLR, but not by loss of function of either single NLR. Elucidation of such models requires further biochemical and structural work on plant NLR self-association interfaces (Zhang et al., 2017) in light of animal NLR oligomerization (Hu et al., 2015).

More than one NLR may contribute to autoimmunity in other mutants, including *acd11* and *mpk4*. For example, *laz5-D2* can fully suppresses *acd11* autoimmunity, although *acd11 laz5-1* doubly homozygous recessive mutants still display significant cell death and activated defense under certain growth conditions (Palma et al., 2010). Similarly, *summ2* only partially suppresses *mpk4* (Zhang et al., 2012). In addition, some NLRs function in pairs of a sensor and a trigger (Césari et al., 2014; Sarris and Jones, 2015). However, since both DSC1 and DSC2 can independently trigger immunity in the absence of CAMTA3, it is unlikely they constitute a sensor/trigger pair. It appears more likely that different activities of microbial effectors targeting CAMTA3 or CAMTA3-containing complexes or pathways are differentially sensed by DSC1 and 2. According to the NLR phylogeny of Meyers et al. (2003), DSC1 and DSC2 are not especially closely related. This may not be surprising, however, as two NLRs that monitor RIN4 function, RPS2 and RPM1, are also not especially closely related.

We conclude that our screen to link NLR-DN alleles to potential guardees is a more robust and timely method than suppression screens of double loss-of-function mutants. Furthermore, our dominant-negative method can identify NLRs with redundant functions or working in pairs. If exploited, our collection of NLR-DN constructs (Table S1) should clarify the relationships between guardees and numerous negative regulators of immunity and cell death in plants.

STAR★METHODS

Detailed methods are provided in the online version of this paper and include the following:

- KEY RESOURCES TABLE
- CONTACT FOR REAGENT AND RESOURCE SHARING
- EXPERIMENTAL MODEL AND SUBJECT DETAILS
  - *Arabidopsis thaliana*
  - *Nicotiana benthamiana*
  - *Escherichia coli*
  - *Agrobacterium tumefaciens*
  - *Pseudomonas syringae pv. tomato* DC3000
- METHOD DETAILS
  - Cloning
  - Generation of transgenic *Arabidopsis* lines
  - NLR P loop collection
  - Ion leakage
  - Resistance assay
  - Trypan blue staining
  - Quantitative Real-Time PCR
  - Cell death
  - Subcellular localization and FRET
  - Protein extraction and Co-immunoprecipitation
  - SDS-PAGE and immunoblotting
- QUANTIFICATION AND STATISTICAL ANALYSIS

SUPPLEMENTAL INFORMATION

Supplemental Information includes five figures and two tables and can be found with this article online at http://dx.doi.org/10.1016/j.chom.2017.03.005.

AUTHOR CONTRIBUTIONS

S.L., C.G., K.P., M.R., M.K.J., S.B., E.R., and K.S. performed the experiments. S.L., C.G., J.M., and M.P. designed the experiments. S.L., C.G., J.M., and M.P. wrote the manuscript.

ACKNOWLEDGMENTS

We thank Suksawad Vongvisuttikun for technical help. We thank Tsuyoshi Nakagawa (Shimane University) for providing Gateway binary pGWB vectors. RPS4_HA was kindly provided by Jonathan D.G. Jones (The Sainsbury Laboratory). The *camta1 camta3* double line was a gift from Michael F. Thomashow (Michigan State University). All confocal work was done at the Center for Advanced Bioimaging. This research was supported by a grant to J.M. from the Danish Strategic Research Council (09-067148) and to M.P. from the Danish Council for Independent Research (11-106302).

Received: June 22, 2016
Revised: November 16, 2016
Accepted: March 9, 2017
Published: April 12, 2017

REFERENCES

Aarts, N., Metz, M., Holub, E., Staskawicz, B.J., Daniels, M.J., and Parker, J.E. (1998). Different requirements for EDS1 and NDR1 by disease resistance genes define at least two R gene-mediated signaling pathways in Arabidopsis. Proc. Natl. Acad. Sci. USA *95*, 10306–10311.

Axtell, M.J., and Staskawicz, B.J. (2003). Initiation of RPS2-specified disease resistance in Arabidopsis is coupled to the AvrRpt2-directed elimination of RIN4. Cell *112*, 369–377.

Belkhadir, Y., Nimchuk, Z., Hubert, D.A., Mackey, D., and Dangl, J.L. (2004). Arabidopsis RIN4 negatively regulates disease resistance mediated by RPS2 and RPM1 downstream or independent of the NDR1 signal modulator and is not required for the virulence functions of bacterial type III effectors AvrRpt2 or AvrRpm1. Plant Cell *16*, 2822–2835.

Benn, G., Bjornson, M., Ke, H., De Souza, A., Balmond, E.I., Shaw, J.T., and Dehesh, K. (2016). Plastidial metabolite MEcPP induces a transcriptionally centered stress-response hub via the transcription factor CAMTA3. Proceedings of the National Academy of Sciences of the United States of America *113*, 8855–8860.

Benn, G., Wang, C.Q., Hicks, D.R., Stein, J., Guthrie, C., and Dehesh, K. (2014). A key general stress response motif is regulated non-uniformly by CAMTA transcription factors. Plant J. *80*, 82–92.

Bent, A.F., Kunkel, B.N., Dahlbeck, D., Brown, K.L., Schmidt, R., Giraudat, J., Leung, J., and Staskawicz, B.J. (1994). RPS2 of Arabidopsis thaliana: a leucine-rich repeat class of plant disease resistance genes. Science *265*, 1856–1860.

Bjornson, M., Benn, G., Song, X., Comai, L., Franz, A.K., Dandekar, A.M., Drakakaki, G., and Dehesh, K. (2014). Distinct roles for mitogen-activated protein kinase signaling and CALMODULIN-BINDING TRANSCRIPTIONAL ACTIVATOR3 in regulating the peak time and amplitude of the plant general stress response. Plant Physiol. *166*, 988–996.

Bomblies, K., and Weigel, D. (2007). Arabidopsis: a model genus for speciation. Curr. Opin. Genet. Dev. *17*, 500–504.

Bonardi, V., Tang, S., Stallmann, A., Roberts, M., Cherkis, K., and Dangl, J.L. (2011). Expanded functions for a family of plant intracellular immune receptors beyond specific recognition of pathogen effectors. Proc. Natl. Acad. Sci. USA *108*, 16463–16468.

Bouché, N., Scharlat, A., Snedden, W., Bouchez, D., and Fromm, H. (2002). A novel family of calmodulin-binding transcription activators in multicellular organisms. J. Biol. Chem. *277*, 21851–21861.

Brodersen, P., Petersen, M., Pike, H.M., Olszak, B., Skov, S., Odum, N., Jørgensen, L.B., Brown, R.E., and Mundy, J. (2002). Knockout of Arabidopsis accelerated-cell-death11 encoding a sphingosine transfer protein causes activation of programmed cell death and defense. Genes Dev. *16*, 490–502.

Brodersen, P., Petersen, M., Bjørn Nielsen, H., Zhu, S., Newman, M.A., Shokat, K.M., Rietz, S., Parker, J., and Mundy, J. (2006). Arabidopsis MAP kinase 4 regulates salicylic acid- and jasmonic acid/ethylene-dependent responses via EDS1 and PAD4. Plant J. *47*, 532–546.

Bruggeman, Q., Raynaud, C., Benhamed, M., and Delarue, M. (2015). To die or not to die? Lessons from lesion mimic mutants. Front. Plant Sci. *6*, 24.

Buell, C.R., Joardar, V., Lindeberg, M., Selengut, J., Paulsen, I.T., Gwinn, M.L., Dodson, R.J., Deboy, R.T., Durkin, A.S., Kolonay, J.F., et al. (2003). The complete genome sequence of the Arabidopsis and tomato pathogen Pseudomonas syringae pv. tomato DC3000. Proc. Natl. Acad. Sci. USA *100*, 10181–10186.

Century, K.S., Holub, E.B., and Staskawicz, B.J. (1995). NDR1, a locus of Arabidopsis thaliana that is required for disease resistance to both a bacterial and a fungal pathogen. Proceedings of the National Academy of Sciences of the United States of America *92*, 6597–6601.

Césari, S., Kanzaki, H., Fujiwara, T., Bernoux, M., Chalvon, V., Kawano, Y., Shimamoto, K., Dodds, P., Terauchi, R., and Kroj, T. (2014). The NB-LRR proteins RGA4 and RGA5 interact functionally and physically to confer disease resistance. EMBO J. *33*, 1941–1959.

Chae, E., Bomblies, K., Kim, S.T., Karelina, D., Zaidem, M., Ossowski, S., Martín-Pizarro, C., Laitinen, R.A., Rowan, B.A., Tenenboim, H., et al. (2014). Species-wide genetic incompatibility analysis identifies immune genes as hot spots of deleterious epistasis. Cell *159*, 1341–1351.

Chung, E.H., da Cunha, L., Wu, A.J., Gao, Z., Cherkis, K., Afzal, A.J., Mackey, D., and Dangl, J.L. (2011). Specific threonine phosphorylation of a host target by two unrelated type III effectors activates a host innate immune receptor in plants. Cell Host Microbe *9*, 125–136.

Clough, S.J., and Bent, A.F. (1998). Floral dip: a simplified method for Agrobacterium-mediated transformation of Arabidopsis thaliana. Plant J. *16*, 735–743.

Dangl, J.L., Horvath, D.M., and Staskawicz, B.J. (2013). Pivoting the plant immune system from dissection to deployment. Science *341*, 746–751.

DeYoung, B.J., and Innes, R.W. (2006). Plant NBS-LRR proteins in pathogen sensing and host defense. Nat. Immunol. *7*, 1243–1249.

Dietrich, R.A., Delaney, T.P., Uknes, S.J., Ward, E.R., Ryals, J.A., and Dangl, J.L. (1994). Arabidopsis mutants simulating disease resistance response. Cell *77*, 565–577.

Dinesh-Kumar, S.P., Tham, W.H., and Baker, B.J. (2000). Structure-function analysis of the tobacco mosaic virus resistance gene N. Proc. Natl. Acad. Sci. USA *97*, 14789–14794.

Doherty, C.J., Van Buskirk, H.A., Myers, S.J., and Thomashow, M.F. (2009). Roles for Arabidopsis CAMTA transcription factors in cold-regulated gene expression and freezing tolerance. Plant Cell *21*, 972–984.

Du, L., Ali, G.S., Simons, K.A., Hou, J., Yang, T., Reddy, A.S., and Poovaiah, B.W. (2009). Ca(2+)/calmodulin regulates salicylic-acid-mediated plant immunity. Nature *457*, 1154–1158.

Eitas, T.K., and Dangl, J.L. (2010). NB-LRR proteins: pairs, pieces, perception, partners, and pathways. Curr. Opin. Plant Biol. *13*, 472–477.

Eitas, T.K., Nimchuk, Z.L., and Dangl, J.L. (2008). Arabidopsis TAO1 is a TIR-NB-LRR protein that contributes to disease resistance induced by the Pseudomonas syringae effector AvrB. Proc. Natl. Acad. Sci. USA *105*, 6475–6480.

Galon, Y., Nave, R., Boyce, J.M., Nachmias, D., Knight, M.R., and Fromm, H. (2008). Calmodulin-binding transcription activator (CAMTA) 3 mediates biotic defense responses in Arabidopsis. FEBS Lett. *582*, 943–948.

Geu-Flores, F., Nour-Eldin, H.H., Nielsen, M.T., and Halkier, B.A. (2007). USER fusion: a rapid and efficient method for simultaneous fusion and cloning of multiple PCR products. Nucleic Acids Res. *35*, e55.

Gómez-Gómez, L., and Boller, T. (2002). Flagellin perception: a paradigm for innate immunity. Trends Plant Sci. *7*, 251–256.

Grant, M.R., Godiard, L., Straube, E., Ashfield, T., Lewald, J., Sattler, A., Innes, R.W., and Dangl, J.L. (1995). Structure of the Arabidopsis RPM1 gene enabling dual specificity disease resistance. Science *269*, 843–846.

Grant, M., Brown, I., Adams, S., Knight, M., Ainslie, A., and Mansfield, J. (2000). The RPM1 plant disease resistance gene facilitates a rapid and sustained increase in cytosolic calcium that is necessary for the oxidative burst and hypersensitive cell death. Plant J. *23*, 441–450.

Greenberg, J.T., and Ausubel, F.M. (1993). Arabidopsis mutants compromised for the control of cellular damage during pathogenesis and aging. Plant J. *4*, 327–341.

Greenberg, J.T., Guo, A., Klessig, D.F., and Ausubel, F.M. (1994). Programmed cell death in plants: a pathogen-triggered response activated coordinately with multiple defense functions. Cell *77*, 551–563.

Hinsch, M., and Staskawicz, B. (1996). Identification of a new Arabidopsis disease resistance locus, RPs4, and cloning of the corresponding avirulence gene, avrRps4, from Pseudomonas syringae pv. pisi. Mol. Plant Microbe Interact *9*, 55–61.

Hu, Z., Zhou, Q., Zhang, C., Fan, S., Cheng, W., Zhao, Y., Shao, F., Wang, H.W., Sui, S.F., and Chai, J. (2015). Structural and biochemical basis for induced self-propagation of NLRC4. Science *350*, 399–404.

Jing, B., Xu, S., Xu, M., Li, Y., Li, S., Ding, J., and Zhang, Y. (2011). Brush and spray: a high-throughput systemic acquired resistance assay suitable for large-scale genetic screening. Plant Physiology *157*, 973–980.

Jones, J.D., and Dangl, J.L. (2006). The plant immune system. Nature *444*, 323–329.

Kim, Y., Park, S., Gilmour, S.J., and Thomashow, M.F. (2013). Roles of CAMTA transcription factors and salicylic acid in configuring the low-temperature transcriptome and freezing tolerance of Arabidopsis. Plant J. *75*, 364–376.

Koncz, C., and Schell, J. (1986). The promoter of Tl-DNA gene 5 controls the tissue-specific expression of chimeric genes carried by a novel type of agrobacterium binary vector. J. Molec. Gen. Genet. *204*, 383–396.

Lazo, G.R., Stein, P.A., and Ludwig, R.A. (1991). A DNA transformation-competent Arabidopsis genomic library in agrobacterium. Biotechnology *9*, 963–967.

Leipe, D.D., Koonin, E.V., and Aravind, L. (2004). STAND, a class of P-loop NTPases including animal and plant regulators of programmed cell death: multiple, complex domain architectures, unusual phyletic patterns, and evolution by horizontal gene transfer. J. Mol. Biol. *343*, 1–28.

Lu, D., Lin, W., Gao, X., Wu, S., Cheng, C., Avila, J., Heese, A., Devarenne, T.P., He, P., and Shan, L. (2011). Direct ubiquitination of pattern recognition receptor FLS2 attenuates plant innate immunity. Science *332*, 1439–1442.

Mackey, D., Belkhadir, Y., Alonso, J.M., Ecker, J.R., and Dangl, J.L. (2003). Arabidopsis RIN4 is a target of the type III virulence effector AvrRpt2 and modulates RPS2-mediated resistance. Cell *112*, 379–389.

Mestre, P., and Baulcombe, D.C. (2006). Elicitor-mediated oligomerization of the tobacco N disease resistance protein. Plant Cell *18*, 491–501.

Meyers, B.C., Kozik, A., Griego, A., Kuang, H., and Michelmore, R.W. (2003). Genome-wide analysis of NBS-LRR-encoding genes in Arabidopsis. Plant Cell *15*, 809–834.

Nakagawa, T., Kurose, T., Hino, T., Tanaka, K., Kawamukai, M., Niwa, Y., Toyooka, K., Matsuoka, K., Jinbo, T., and Kimura, T. (2007). Development of series of gateway binary vectors, pGWBs, for realizing efficient construction of fusion genes for plant transformation. J. Biosci. Bioeng. *104*, 34–41.

Narusaka, M., Shirasu, K., Noutoshi, Y., Kubo, Y., Shiraishi, T., Iwabuchi, M., and Narusaka, Y. (2009). RRS1 and RPS4 provide a dual Resistance-gene system against fungal and bacterial pathogens. Plant J. *60*, 218–226.

Narusaka, M., Kubo, Y., Hatakeyama, K., Imamura, J., Ezura, H., Nanasato, Y., Tabei, Y., Takano, Y., Shirasu, K., and Narusaka, Y. (2013). Interfamily transfer of dual NB-LRR genes confers resistance to multiple pathogens. PLoS ONE *8*, e55954.

Nie, H., Zhao, C., Wu, G., Wu, Y., Chen, Y., and Tang, D. (2012). SR1, a calmodulin-binding transcription factor, modulates plant defense and ethylene-induced senescence by directly regulating NDR1 and EIN3. Plant Physiol. *158*, 1847–1859.

Norholm, M.H. (2010). A mutant Pfu DNA polymerase designed for advanced uracil-excision DNA engineering. BMC Biotechnol. *10*, 21.

Nour-Eldin, H.H., Hansen, B.G., Norholm, M.H., Jensen, J.K., and Halkier, B.A. (2006). Advancing uracil-excision based cloning towards an ideal technique for cloning PCR fragments. Nucleic Acids Res. *34*, e122.

Palma, K., Thorgrimsen, S., Malinovsky, F.G., Fiil, B.K., Nielsen, H.B., Brodersen, P., Hofius, D., Petersen, M., and Mundy, J. (2010). Autoimmunity in Arabidopsis acd11 is mediated by epigenetic regulation of an immune receptor. PLoS Pathog. *6*, e1001137.

Parker, J.E., Holub, E.B., Frost, L.N., Falk, A., Gunn, N.D., and Daniels, M.J. (1996). Characterization of eds1, a mutation in Arabidopsis suppressing resistance to Peronospora parasitica specified by several different RPP genes. Plant Cell *8*, 2033–2046.

Petersen, M., Brodersen, P., Naested, H., Andreasson, E., Lindhart, U., Johansen, B., Nielsen, H.B., Lacy, M., Austin, M.J., Parker, J.E., et al. (2000). Arabidopsis map kinase 4 negatively regulates systemic acquired resistance. Cell *103*, 1111–1120.

Roberts, M., Tang, S., Stallmann, A., Dangl, J.L., and Bonardi, V. (2013). Genetic requirements for signaling from an autoactive plant NB-LRR intracellular innate immune receptor. PLoS Genet. *9*, e1003465.

Rodriguez, E., El Ghoul, H., Mundy, J., and Petersen, M. (2016). Making sense of plant autoimmunity and 'negative regulators'. FEBS J. *283*, 1385–1391.

Roux, M.E., Rasmussen, M.W., Palma, K., Lolle, S., Regué, A.M., Bethke, G., Glazebrook, J., Zhang, W., Sieburth, L., Larsen, M.R., et al. (2015). The mRNA decay factor PAT1 functions in a pathway including MAP kinase 4 and immune receptor SUMM2. EMBO J. *34*, 593–608.

Sarris, P.F., and Jones, J.D. (2015). Plant immune receptors mimic pathogen virulence targets. Oncotarget *6*, 16824–16825.

Saucet, S.B., Ma, Y., Sarris, P.F., Furzer, O.J., Sohn, K.H., and Jones, J.D. (2015). Two linked pairs of Arabidopsis TNL resistance genes independently confer recognition of bacterial effector AvrRps4. Nat. Commun. *6*, 6338.

Shirano, Y., Kachroo, P., Shah, J., and Klessig, D.F. (2002). A gain-of-function mutation in an Arabidopsis Toll Interleukin1 receptor-nucleotide binding site-leucine-rich repeat type R gene triggers defense responses and results in enhanced disease resistance. Plant Cell *14*, 3149–3162.

Simanshu, D.K., Zhai, X., Munch, D., Hofius, D., Markham, J.E., Bielawski, J., Bielawska, A., Malinina, L., Molotkovsky, J.G., Mundy, J.W., et al. (2014). Arabidopsis accelerated cell death 11, ACD11, is a ceramide-1-phosphate transfer protein and intermediary regulator of phytoceramide levels. Cell Rep. *6*, 388–399.

Sohn, K.H., Segonzac, C., Rallapalli, G., Sarris, P.F., Woo, J.Y., Williams, S.J., Newman, T.E., Paek, K.H., Kobe, B., and Jones, J.D. (2014). The nuclear immune receptor RPS4 is required for RRS1SLH1-dependent constitutive defense activation in Arabidopsis thaliana. PLoS Genet. *10*, e1004655.

Speth, E.B., Lee, Y.N., and He, S.Y. (2007). Pathogen virulence factors as molecular probes of basic plant cellular functions. Curr. Opin. Plant Biol. *10*, 580–586.

Spoel, S.H., and Dong, X. (2012). How do plants achieve immunity? Defence without specialized immune cells. Nat. Rev. Immunol. *12*, 89–100.

Tornero, P., Chao, R.A., Luthin, W.N., Goff, S.A., and Dangl, J.L. (2002). Large-scale structure-function analysis of the Arabidopsis RPM1 disease resistance protein. Plant Cell *14*, 435–450.

Tsuda, K., Mine, A., Bethke, G., Igarashi, D., Botanga, C.J., Tsuda, Y., Glazebrook, J., Sato, M., and Katagiri, F. (2013). Dual regulation of gene expression mediated by extended MAPK activation and salicylic acid contributes to robust innate immunity in Arabidopsis thaliana. PLoS Genet. *9*, e1004015.

Walley, J.W., Coughlan, S., Hudson, M.E., Covington, M.F., Kaspi, R., Banu, G., Harmer, S.L., and Dehesh, K. (2007). Mechanical stress induces biotic and abiotic stress responses via a novel cis-element. PLoS Genet. *3*, 1800–1812.

Zhang, Y., Goritschnig, S., Dong, X., and Li, X. (2003). A gain-of-function mutation in a plant disease resistance gene leads to constitutive activation of downstream signal transduction pathways in suppressor of npr1-1, constitutive 1. Plant Cell *15*, 2636–2646.

Zhang, Y., Dorey, S., Swiderski, M., and Jones, J.D. (2004). Expression of RPS4 in tobacco induces an AvrRps4-independent HR that requires EDS1, SGT1 and HSP90. Plant J. *40*, 213–224.

Zhang, Z., Wu, Y., Gao, M., Zhang, J., Kong, Q., Liu, Y., Ba, H., Zhou, J., and Zhang, Y. (2012). Disruption of PAMP-induced MAP kinase cascade by a Pseudomonas syringae effector activates plant immunity mediated by the NB-LRR protein SUMM2. Cell Host Microbe *11*, 253–263.

Zhang, X., Bernoux, M., Bentham, A.R., Newman, T.E., Ve, T., Casey, L.W., Raaymakers, T.M., Hu, J., Croll, T.I., Schreiber, K.J., et al. (2017). Multiple functional self-association interfaces in plant TIR domains. Proc. Natl. Acad. Sci. USA *114*, E2046–E2052.

STAR★METHODS

KEY RESOURCES TABLE

REAGENT or RESOURCE	SOURCE	IDENTIFIER
Antibodies		
Mouse monoclonal αHA-prope (F-7)	Santa Cruz Biotechnology	Cat# sc-7392; RRID:AB_627809
Mouse HA-Tag (6E2) mAb	Cell Signaling Technology	Cat# 2367S; RRID:AB_10691311
Rabbit anti GFP pAb (TP401)	AMSBIO LLC	Cat# TP401; RRID:AB_10890443
Anti-Rabbit IgG (H+L), HRP Conjugate antibody	Promega	Cat# W4011; RRID:AB_430833
Anti-Mouse IgG (H+L), HRP Conjugate antibody	Promega	Cat# W4021; RRID:AB_430834
Anti-Rabbit IgG (Fc), AP Conjugate antibody	Promega	Cat# S3731; RRID:AB_430872
Anti-Mouse IgG (H+L), AP Conjugate antibody	Promega	Cat# S3721; RRID:AB_430871
EZview Red Protein A Affinity Gel	SIGMA-ALDRICH	P6486
Lama GFP-Trap_A monoclonal	Chromo Tek	Cat# gta-20; RRID:AB_2631357
Bacterial and Virus Strains		
Agrobacterium tumefaciens strain GV3101	Koncz and Schell, 1986	N/A
Agrobacterium tumefaciens strain Agl-1	Lazo et al., 1991	N/A
Escherichia coli strain XL-Blue	Stratagene	N/A
Pseudomonas syringae pv. tomato DC3000 (pVSP61)	Century et al., 1995	N/A
Pseudomonas syringae pv. tomato DC3000 (AvrRpm1)	Grant et al., 1995	N/A
Pseudomonas syringae pv. tomato DC3000 (AvrRps4)	Hinsch and Staskawicz, 1996	N/A
Pseudomonas syringae pv. tomato DC3000 (AvrRpt2)	Bent et al., 1994	N/A
Critical Commercial Assays		
NucleoSpin RNA II	Macherey-Nagel	Cat# 740955.250
RevertAid First Strand cDNA Synthesis Kit	ThermoFisher Scientific	Cat# K1622
Maxima SYBR Green/ROX qPCR Master Mix (2X)	ThermoFisher Scientific	Cat# K0221
Monarch Plasmid Miniprep Kit	NEW ENGLAND BioLabs	Cat# T1010S
Experimental Models: Organisms/Strains		
Arabidopsis: *camta3*: At2g22300 T-DNA insertion: SALK_001152	Galon et al., 2008 NASC	NASC ID: N501152
Arabidopsis: *dsc1*: At4g12010 T-DNA insertion: Sail_49_C05	NASC	NASC ID: N802333
Arabidopsis: *dsc2*: At5g18370 T-DNA insertion: FLAG_014A11	Versailles *Arabidopsis* Stock Center	COMTV9T3
Arabidopsis: *camta3 dsc1*: SALK_001152, Sail_49_C05 T-DNA insertion	This paper	N/A
Arabidopsis: *camta3 dsc2*: SALK_001152, FLAG_014A11 T-DNA insertion	This paper	N/A
Arabidopsis: *camta3 dsc1 dsc2*: SALK_001152, Sail_49_C05, FLAG_014A11 T-DNA insertion	This paper	N/A
Arabidopsis: *camta1 camta3*: At5g09410, At2g22300 T-DNA insertion: SALK_008187, SALK_001152	Doherty et al., 2009	N/A
Arabidopsis: *DSC1-DN*: At4g12010 GKT(T/S) - > AAT(T/S)	This paper	N/A
Arabidopsis: *DSC2-DN*: At5g18370 GKT(T/S) - > AAT(T/S)	This paper	N/A
Arabidopsis: *camta3 DSC1-DN*: SALK_001152, At4g12010 GKT(T/S) - > AAT(T/S)	This paper	N/A
Arabidopsis: *camta3 DSC2-DN*: SALK_001152, At5g18370 GKT(T/S) - > AAT(T/S)	This paper	N/A
Arabidopsis: *camta1 camta3 DSC1-DN*: SALK_008187, SALK_001152, At4g12010 GKT(T/S) - > AAT(T/S)	This paper	N/A
Arabidopsis: *rpm1-3*: At3g07040 T1157A - > Y87STOP:	Grant et al., 1995	NASC ID: N68739
Arabidopsis: *eds1-2*: At3g48090 900bp deletion	Aarts et al., 1998	N/A

(*Continued on next page*)

Continued		
REAGENT or RESOURCE	SOURCE	IDENTIFIER
Arabidopsis: *ndr1-1*: At3g20600	Century et al., 1995	N/A
Arabidopsis: *pat1-1*: At1g79090 T-DNA insertion: SALK_040660	Roux et al., 2015 NASC	NASC ID: N657369
Arabidopsis: *summ2-8*: At1g12280 T-DNA insertion: SAIL_1152_A06	Zhang et al., 2012 NASC	NASC ID: N842411
Arabidopsis: pat1 summ2: At1g79090, At1g12280 T-DNA insertion	Roux et al., 2015	N/A
Oligonucleotides		
Primers for qPCR, see Table S2	This paper; Roux et al., 2015	N/A
Primers for genotyping, see Table S2	This paper; Roux et al., 2015	N/A
Primers for cloning, see Table S2	This paper	N/A
Recombinant DNA		
P-loop mutated NLRs, see Table S1	This paper	N/A
CAMTA1(At5g09410) in pENTR/D-TOPO	ABRC Stock	TOPO-U21-C07
CAMTA2 (At5g64220) in pENTR/D-TOPO	ABRC Stock	TOPO-U19-B06
pBin19 g-35S:RPS4-HA	Zhang et al., 2004	N/A
pGWBs	Nakagawa et al., 2007	N/A
pENTRU: pENTR modified for USER cloning	This paper	N/A
pENTRU_CAMTA3 (gDNA -STOP)	This paper	N/A
pENTRU_DSC1 (gDNA -STOP)	This paper	N/A
pENTRU_DSC2 (gDNA -STOP)	This paper	N/A
35S::CAMTA3_HA (pGWB514)	This paper	N/A
35S::CFP_CAMTA3 (pGWB645)	This paper	N/A
35S::HA_DSC1 (pGWB515)	This paper	N/A
35S::YFP_DSC1 (pGWB542)	This paper	N/A
35S::DSC2_YFP (pGWB541)	This paper	N/A
35S::YFP_DSC2 (pGWB542)	This paper	N/A
35S::GFP_MYC (pGWB517)	This paper	N/A
35S::CFP_CAMTA1 (pGWB645)	This paper	N/A
35S::CFP_CAMTA2 (pGWB645)	This paper	N/A

CONTACT FOR REAGENT AND RESOURCE SHARING

Further information and requests for resources and reagents should be directed to and will be fulfilled by the Lead Contact, Morten Petersen (shutko@bio.ku.dk).

EXPERIMENTAL MODEL AND SUBJECT DETAILS

Arabidopsis thaliana

Arabidopsis plants were grown in 9 × 9 cm pots in growth chambers at 22°C and ~70% relative humidity and with an 8 hr photoperiod. The intensity of the light was set at ~140 μE $m^{-2}s^{-1}$. The following *Arabidopsis* lines were used in this study: wild-type Colombia (Col-0), camta3-1 (referred to as camta3), SALK_001152 (Galon et al., 2008); *dsc1*, Sail_49_C05; *dsc2*, SALK_009668; *rpm1-3* (Grant et al., 1995); *pat1-1*, *summ2-8* (Zhang et al., 2012); *pat1/summ2* (Roux et al., 2015); *ndr1-1* (Century et al., 1995) and *eds1-2* (Parker et al., 1996; Aarts et al., 1998). All lines have been authenticated by genotyping; the primers used are listed in Table S2. All P loop mutated NLR lines created in this study is listed in Table S1.

Nicotiana benthamiana

Plants were grown in greenhouses under controlled conditions (24°C and 40%–65% relative humidity), and a long-day photoperiod (16 hr light and 8 hr dark). Illumination were set to ~130-150 μE m^{-2} sec^{-1}.

Escherichia coli

E.coli (XL blue) were grown on LB plates with appropriate antibiotic at 37°C and kept at 4°C for up to two weeks. For liquid cultures a bacterial scrape were inoculated in 5 mL LB supplemented with appropriate antibiotics and grown at 37°C under shaking.

Agrobacterium tumefaciens

Strains of *Agrobacterium* (GV3101 and Agl-1) were grown on YEP plates with appropriate antibiotic at 28°C and kept at 4°C for up to two weeks. For liquid cultures a bacterial scrape were inoculated in 5 mL YEP supplemented with appropriate antibiotics and grown at 28°C under shaking. After 24 hr, YEP was added to a total volume of 11 ml.

Pseudomonas syringae pv. tomato DC3000

Pst. DC3000 strains were grown on NYG plants containing 100 μg/ml rifampicin, 12.5 mikrogram/ml kanamycin, and 50mikrogram/ml cyclohexamide at 28°C for two days. For liquid cultures 5 mL NYC supplemented with kanamycin and rifampicin were inoculated with a slab of bacteria. *Pst.* DC3000 containing the avirulence genes avrRpm1 (Grant et al., 1995), avrRps4 (Hinsch and Staskawicz, 1996), avrRpt2 (Bent et al., 1994) in the broad host range vector pVSP61, or DC3000 containing empty pVSP6, were used in this study.

METHOD DETAILS

Cloning

WT CAMTA3, DSC1 and DSC2 was amplified from genomic DNA (from Col-0 plants) without STOP codon and cloned into a modified USER compatible pENTR vector using uracil-excision based cloning (USER, New England Biolabs). Cloning primers were tagged with 5′-ggcttaaU3′ for the forward primer and 5′-ggtttaaU3′ for the reverse primer. Constructs were transferred to Gateway-compatible constitutive expression vectors by LR recombination reaction (Invitrogen). Plasmids were verified by sequencing and then electroporated into *Agrobacterium tumefaciens* GV3101.

For subcellular localization, FRET, cell death and immunoprecipitation, CAMTA3 were transferred to pGWB645 (35S pro, N-terminal CFP) and pGWB514 (35S pro, C-terminal HA); DSC1 were transferred to pGWB542 (35S pro, N-terminal YFP) and pGWB515 (35S pro, N-terminal HA) and DSC2 were transferred to pGWB541 (35S pro, C-terminal YFP) and pGWB542.

GFP was PCR amplified from plasmid template and cloned into pENTR/D-TOPO (Invitrogen). The construct was subsequently transferred to the Gateway-compatible constitutive expression vector pGWB517 (35S pro, C-terminal MYC) by LR recombination reaction (Invitrogen). The plasmid were verified by sequencing and then electroporated into *Agrobacterium tumefaciens* Agl-1.

CAMTA1 and CAMTA2 in pENTR/D-TOPO were obtained from the ABRC Stock center. CAMTA1 and CAMTA2 were transferred to pGWB645 (35S pro, N-terminal CFP) by LR recombination reaction (Invitrogen). Plasmids were verified by sequencing and then electroporated into *Agrobacterium tumefaciens* GV3101.

Generation of transgenic *Arabidopsis* lines

To generate the double mutants, *camta3-1* homozygous plants were crossed with homozygous *dsc1* or *dsc2*. Homozygous double mutant plants were identified in the F2 progeny by PCR. For the *camta3/dsc1/dsc2* triple mutant, homozygous *camta3/dsc1* double mutants were crossed with homozygous *camta3/dsc2*. Homozygous triple mutants were identified in the F2 progeny by PCR. Homozygosity and correct insertion T-DNA sites were verified by PCR using standard conditions. Genotyping primers for T-DNA lines are provided in Table S2.

Generation of *camta1 camta3 DSC1-DN* lines was done by genetic crossing of homozygote lines of the *camta1 camta3* double mutants and *DSC1-DN*. Homozygous triple mutants were identified by PCR. Homozygosity and correct insertion T-DNA sites were verified by PCR using standard conditions. Genomic constructs used to complement *camta3 dsc1 dsc2* triple mutants was inserted in pGWB601. Plants were transformed by floral dip (Clough and Bent, 1998).

NLR P loop collection

P loop mutated NLRs were created from genomic DNA by USER mutagenesis (Nour-Eldin et al., 2006) and cloned into a modified USER compatible pCAMBIA-3300, using uracil-excision based cloning (USER, New England Biolabs). Cloning primers were tagged with 5′-ggcttaaU3′ for the forward primer and 5′-ggtttaaU3′ for the reverse primer. Mutagenesis primers were made containing the P loop mutation GXXXXGKT(T/S) to GXXXXAAT(T/S) of the P loop motif and appropriate uracil's incorporated to give seamless overlap of two fragments (Geu-Flores et al., 2007) generated with PfuX7 (Norholm, 2010).

The final constructs were verified by sequencing, electroporated *into Agrobacterium tumefaciens* strain GV3101 and used to transform *camta3* or wild-type plants by the floral dip method (Clough and Bent, 1998). Transgenic plants were selected on soil with BASTA (10 mg/L).

Ion leakage

Four-week-old plants were syringe inoculated with *Pst*. DC3000 (avrRpm1) at OD_{600} = 0.2. Four leaf discs were punched out. Samples were taken from one side of the leaf between the central vein and leaf margin. Leaf discs were washed in distilled H_2O to eliminate signal derived from wounded cells. Four discs from each line were then placed in tubes containing fresh distilled H_2O, and measurements of solution conductivity were taken at the indicated time points using a conductivity meter.

Resistance assay

For bacterial growth assays, leaves of 5-week-old soil grown plants were inoculated by syringe infiltration (OD_{600} = 0.001) with *Pst* DC3000 either containing avirulence genes or the empty vector. Bacterial growth (Colony forming units per cm^2) was determined

3 days post inoculation, day 0 counts were analyzed in infiltrated leaves to ensure that no statistical difference was present at inoculation and that day 3 showed positive growth. The experiments were repeated in at least three individual biological replicates, each with three technical replicates.

Trypan blue staining

Leaves of 6 week-old plants were boiled in Trypan blue 2-3 min and destained in chloral hydrate. Leaves were placed on slides in 50% glycerol for visualization of dead cells.

Quantitative Real-Time PCR

RNA was extracted from plant leaves using the NucleoSpin RNA Plant kit (Machery-Nagel). First-strand cDNA synthesis was carried out using RevertAid First Strand cDNA Synthesis Kit according to the manufacturer's instructions (Thermo Scientific). The constitutively expressed *UBQ10* gene was used as an internal control. qRT-PCR analysis was performed on a Bio-RAD CFX96 system with the dye SYBR Green (Thermo Scientific). All experiments were repeated at least three times each in technical triplicates. Primer sequences are listed in Table S2.

Cell death

For transient expression *N. benthamiana* was syringe infiltrated with *Agrobacterium* at OD_{600} = 0.5 expressing indicated constructs. GV3101 carrying 35S p19 was co-infiltrated at OD_{600} = 0.2. For cell death assays leaves were analyzed ~3 dpi.

Subcellular localization and FRET

N. benthamiana was infiltrated with *Agrobacterium* at OD_{600} = 0.5 expressing indicated constructs. For subcellular localization and FRET, leaf disks were analyzed 2 or 3 dpi. Subcellular localization was done using a LSM700 Zeiss confocal microscope. All samples were imaged with a 63X water objective. The confocal images were edited with Zen2012 (Zeiss) software. FRET-AB was done using a Leica SP5-X inverted confocal microscope. All experiments were done with a 63X water objective. FRET analysis was performed using Leica FRET-AB wizard software.

Protein extraction and Co-immunoprecipitation

N. benthamiana was infiltrated with *Agrobacterium* at OD_{600} = 0.5 expressing indicated constructs. GV3101 carrying 35S p19 was co-infiltrated at OD_{600} = 0.2. Protein were extracted 24 hpi in 50mM Tris-HCl pH 7.5; 150mM NaCl; 10% (v/v) glycerol; 10mM DTT; 10mM EDTA; 0.5% (v/v) PVP; protease inhibitor cocktail (Roche); 0.1% (v/v) Triton X-100 added at 2ml/g tissue powder. Following 20 min centrifugation at 4°C and 13000 rpm sample supernatants were adjusted to ~3mg/ml protein and incubated 2 hr at 4°C with GFPTrap-A beads (Chromotek) or anti-HA antibody (Santa cruz) and EZview protein A agarose beads (Sigma). Beads were washed [20mM Tris pH 7.5; 150mM NaCl; 1mM EDTA] before adding 2x SDS and heating at 80°C.

SDS-PAGE and immunoblotting

Protein samples were separated on 8% SDS-PAGE, electroblotted to PVDF membrane (GE Healthcare), then blocked (1 hr in 5% (w/v) BSA or 5% (w/v) milk in TBS-Tween (0.1%)) and incubated 2 hr to overnight with primary antibodies: anti-GFP 1:5000 (AMS Biotechnology), anti-HA 1:1000 (Santa Cruz), anti-HA 1:1000 (Cell Signaling). Membranes were incubated in secondary antibodies, anti-rabbit or anti-mouse AP or HRP conjugate (Promega; 1:5000) for 1 hr. Chemiluminescent substrate (homemade or ECL Plus, Pierce) was applied before exposure to film (AGFA CP-BU) or camera detection. For AP-conjugated antibodies, membranes were incubated in NBT/BCIP (Roche) until bands were visible.

QUANTIFICATION AND STATISTICAL ANALYSIS

Statistical details of experiments are reported in the figures and figure legends. In short, n = 3 for all samples if nothing else is stated and ± standard deviation of the mean is indicated by error bars. Means not sharing the same letter are significantly different. Statistical significance between groups was determined by ANOVA One-Way comparison followed by Tukey's HSD (honest significant difference) test, $p < 0.05$, was used unless otherwise stated. At least three individual replicas were always included. All statistics were done using the software OriginPro (OriginLab).